J Solid State Electrochem (2011) 15:1885–1891
DOI 10.1007/s10008-010-1207-5

ORIGINAL PAPER

Oscillating oxygen evolution at Ta anodes

Christian Hammer · Benjamin Walther · Hikmet Karabulut · Manuel M. Lohrengel

Received: 15 July 2010 / Revised: 15 September 2010 / Accepted: 20 September 2010 / Published online: 5 October 2010

Abstract Anodic Ta oxide films are said to inhibit oxygen evolution. In industry, however, large amounts of gas are evolved during the anodization of tantalum anodes for electrolytic capacitor fabrication. We quantified the oxygen by fluorescence quenching in a flow-through cuvette and found that 4% of the anodic charge are consumed for oxygen evolution. In wires or sheets, this oxygen is removed by diffusion without bubble formation and, thus, not recognized. Due to the large inner area of the sintered Ta anodes, the oxygen evolution causes strong oscillations of the current density and bubble formation. The amount of oxygen is proportional to the oxide amount formed in parallel. This is explained by a model where mobile ions during oxide growth form interband states which allow electron tunneling. Accordingly, stationary no oxygen evolution is observed.

Keywords Tantalum · Oxygen evolution · Oscillations · Electron tunneling · Fluorescence quenching

Introduction

Valve metals such as Al, Ta, or Nb cover with oxide films in some nanometers in a humid environment, e.g.:

$$4\ Ta + 5\ O_2 \rightarrow 2\ Ta_2O_5 \quad (1)$$

C. Hammer (✉) · B. Walther · M. M. Lohrengel
Institut für Physikalische Chemie,
Heinrich-Heine-University of Duesseldorf,
Universitätsstraße 1,
40225 Düsseldorf, Germany
e-mail: Christian.hammer@uni-duesseldorf.de

H. Karabulut
HC Starck GmbH,
Goslar, Germany

or anodically according to:

$$2\ Ta + 5\ H_2O \rightarrow Ta_2O_5 + 10\ H^+ + 10\ e^- \quad (2)$$

These oxides are similar to ceramics due to their large band gap of 3 to 6 eV. Accordingly, they are perfect insulators for electron transport; ionic movement for oxide growth is only possible due to the extreme field strengths of up to 10 MV cm^{-1} by a special hopping mechanism with activation energies around 2 eV. Therefore, oxygen evolution, which requires an electronic conductivity, should be excluded. In fact, no significant oxygen bubbles are formed in a common experiment with electrode wires or sheets. The current efficiency for anodic oxide formation is >98%, which is reported in the former literature [1, 2].

This result, however, is in contrasts to industrial findings, when large amounts of gas are evolved during the anodization of tantalum anodes for electrolytic capacitor fabrication. Obviously a reaction such as

$$2\ H_2O \rightarrow O_2 + 4\ H^+ + 4\ e^- \quad (3)$$

must be possible. Another reaction which produces gas is the chemical hydrogen formation of base metals in acid solutions, e.g.,

$$2\ Ta + 10\ H^+ \rightarrow 2\ Ta^{5+} + 5\ H_2 \quad (4)$$

This reaction is less probable at anodic potentials, but not impossible if the oxide film shows local break-downs. The aim of this paper is to find out, if and under which conditions oxygen is formed and to identify the gas qualitatively and quantitatively.

High-field oxide growth

The formation of oxide films follows the high-field law [3], which correlates the current density i with the electric field strength E inside the oxide film,

$$i = \nu\rho a \cdot \exp\left(-\frac{W}{RT}\right) \cdot \exp\left(\frac{\alpha azFE}{RT}\right) \quad (5)$$

where z is the charge number and ρ is the charge density of mobile ions, a is the distance of hopping, ν is the oscillation frequency of the ions, (about $6{\cdot}10^{12}$ s^{-1} at room temperature), W is the activation energy, and α is a symmetry factor of the energy barrier. Equation 5 is often abbreviated:

$$i = i_0 \cdot \exp(\beta E) \quad (6)$$

The field strength E is determined by the potential drop ΔU within the oxide film and its thickness d:

$$E = \frac{\Delta U}{d} \quad (7)$$

This potential drop ΔU is calculated from the electrochemical potential by U

$$\Delta U = U - U_0 \quad (8)$$

where U_0 is the zero field potential or the flat band potential, which is normally very close to the equilibrium potential of the oxide electrode, for Ta $U_0 \approx -0.8$ V [4, 5].

Equation 5 and Faraday's law yield the time-dependent oxide growth according to [4]

$$\frac{\partial d}{\partial t} = \frac{M}{\chi y F} \cdot i_0 \exp\left(\beta \frac{\Delta U}{d}\right) \quad (9)$$

with the molecular mass M and the density χ of the anodic oxide; y is the number of electrons required to form one molecule of oxide (e.g., 10 in Eq. 2). Densities χ around 8.5 $g cm^{-3}$ were reported [6–8].

A cyclovoltammogram can be simulated by a simple numeric integration of Eq. 9 (Fig. 1) and corresponds to the experimental one. Typical cyclovoltamograms with 100 $mV s^{-1}$ show no anodic current up to a potential given by the initial oxide film thickness and then a steep rise to the plateau current of oxide formation of 300 $\mu A cm^{-2}$. This current is independent of the potential, and thus, according to Eq. 6, the field strength must be constant during potentiostatic growth, e.g., 6.3 MV cm^{-1} in Fig. 1. This means that the oxide layer thickness d increases linearly with the potential U according to

$$d = k(U - U_0) \quad (10)$$

with an oxide specific film formation factor k. A plateau current density of 300 $\mu A cm^{-2}$ and a composition Ta_2O_5 with a molecular mass of 441.9 g mol^{-1} and a density of 8.5 g cm^{-3} yields k=1.62 $nm V^{-1}$ at 100 $mV s^{-1}$.

The use of Ta capacitors indicates that the anodic oxide represents a perfect dielectric medium. Ta-Metal and electrolyte form the plates of a parallel plate condenser. The capacity C' or the capacity density C is given by:

$$C' = A \cdot \varepsilon \cdot \varepsilon_0 / d \quad (11)$$

$$C = \varepsilon \cdot \varepsilon_0 / d \quad (12)$$

where A is the surface area, ε is the relative dielectric number, ε_0 is the dielectric number of vacuum and d is the distance of the plates, in our case, the oxide thickness. Values for ε around 27 were reported [9–11].

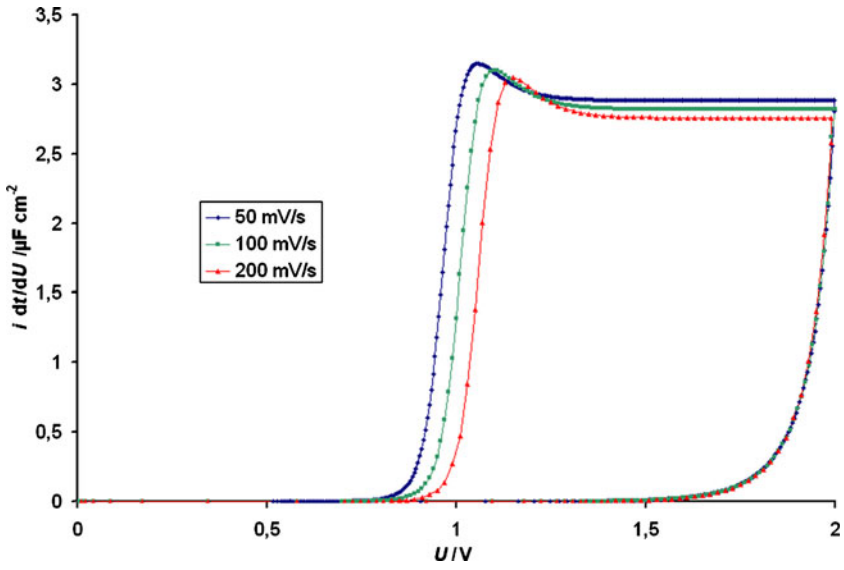

Fig. 1 Simulated cyclovoltammograms of Ta with different dU/dt. Initial oxide thickness d_0=3 nm

If a constant and notable part of the anodic current would produce oxygen, we would expect:

- oxygen is always evolved during oxide formation;
- the current density i_{O2} is proportional to i_{ox};
- i_{O2} is independent of the potential.

Experimental

In former times, oxygen was identified by the formation of bubbles at anodic potentials in most cases. The lack of bubble formation at Ta wire or sheet electrodes lead to the assumption that no oxygen is anodically formed, i.e., the partial current density of oxygen formation must be smaller than some $\mu A cm^{-2}$. Furthermore, the correspondence between anodic charge and oxide film capacity (Eq. 12) indicated that the oxygen current density must be smaller than some percentage of the total anodic current. To quantify the analysis, some problems had to be solved: the amount of oxygen had to be increased up to detectable amounts, and a reliable and applicable technique of oxygen detection had to be developed. The first problem was solved by using Ta electrodes with a large surface, especially porous sintered Ta anodes as used for fabrication of electrolytic capacitors. These anodes had volumes of about 1 mm³ and electrochemically active surfaces of 50 to 300 cm^2. The quantitative analysis of oxygen was done by fluorescence quenching of a special dye, a technique which was refined in our laboratory to quantify the oxygen formation during Electrochemical Machining at extremely large current densities [12].

Ta electrodes

The Ta anodes were made of extremely pure metal and contained less than two·10^{18} cm^{-3} of impurity atoms. The sintered Ta was delivered by H.C. Starck GmbH & Co. KG, Goslar, Germany and formed porous blocks (1×1×1 mm) with a total surface around 100 cm², equipped with a thin Ta wire for contact. The inner active surface was calculated from the plateau currents around 3 V, assuming 300 μA cm^{-2} for a smooth surface at 100 $mV s^{-1}$. Most experiments were carried out in sulphuric acid (3 mol l^{-1}) to get a high conductivity and to minimize the electrolyte resistance in the pores of the sintered anode. The setup for fluorescence quenching, however, required a less aggressive electrolyte.

Fluorescence quenching

Oxygen evolution was quantified by fluorescence quenching of a dye in a flow-through cuvette. The electrolyte consisted of 250 g L^{-1} sodium nitrate p.a. at pH 7 with 0.1 g L^{-1} dichlorotris(1,10-phenanthroline)ruthenium(II) hydrate (98%) as the fluorescence dye.

The solution was thermostated at room temperature and purged with argon gas to remove initial oxygen. A micro-gear pump moved the electrolyte through the cell, a small glass tube with a diameter of about 1 mm which contained the tantalum anode. The electrolyte washed all reaction products into the flow-through cuvette. A blue LED with a wavelength of 447 nm excited the dye and the emission light was directed to the detector (UV–VIS EPP2000, Stellarnet Inc.). A reducing valve behind the cuvette increases the pressure on the right side of Fig. 2 to avoid the formation of bubbles and to keep the generated oxygen solved.

Figure 3 shows excitation and emission spectra of the Ru (II)-phenanthroline-complex with a concentration of 0.01 g L^{-1} in water. The blue curve shows the excitation spectrum at 598 nm. A maximum occurs close to 447 nm, which is just the wavelength of the blue LED used for excitation.

The emission spectrum at 445 nm has its maximum at 598 nm. Between excitation and emission wavelength is a huge stokes-shift, which makes the use of optical filters redundant.

For better fluorescence detection while using the flow-through cuvette, the concentration of the dye was increased to 0.1 g L^{-1}. This concentration caused the best ratio

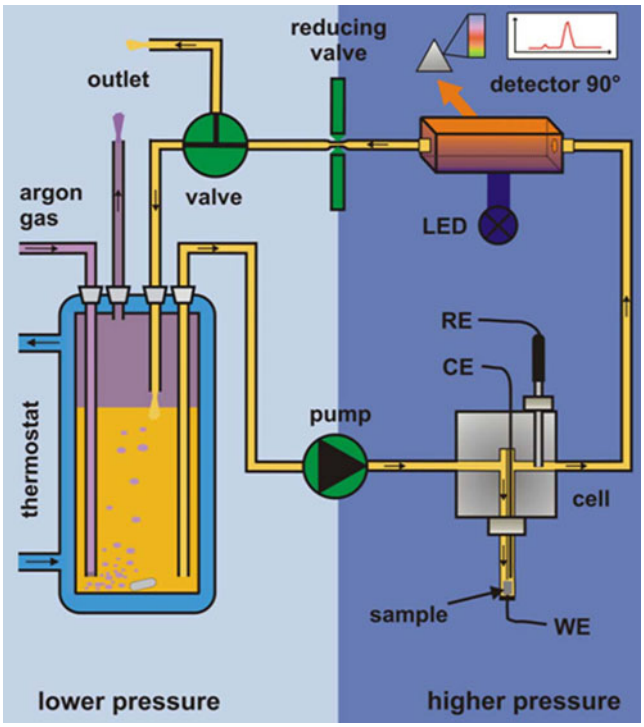

Fig. 2 Scheme of the experimental setup for oxygen quantification [12]

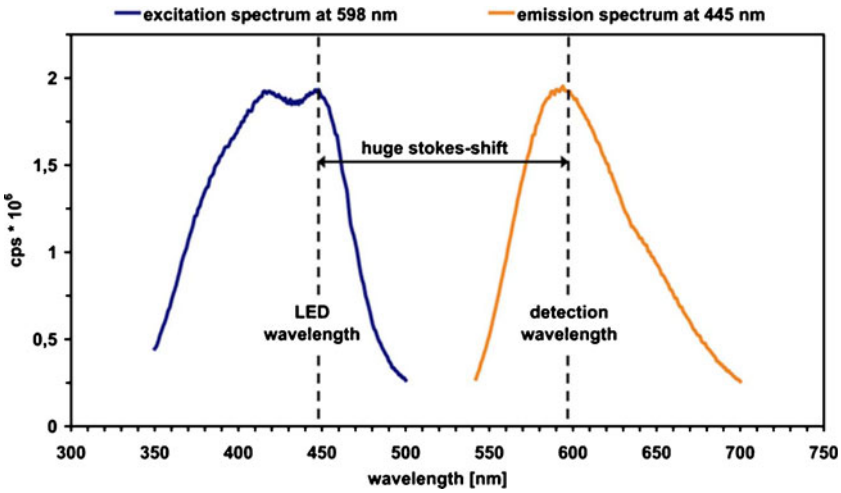

Fig. 3 Excitation and emission spectrum of 0.01 gL^{-1} dichlotris (1,10-phenanthroline)ruthenium (II)hydrate, (98%), in deaerated water

between absorption of the excitation light and intensity of the fluorescence signal. Figure 4 shows the spectra for this concentration. The maximum of the fluorescence signal is about 2,460 counts, if the solution is free of oxygen. The presence of 250 g L^{-1} sodium nitrate does not interfere. If the solution is saturated with oxygen, the dye will be quenched and the intensity of the emitted light decreases to 400 counts. The quenching of the dye is smaller, if sodium nitrate is present. This is no interference, but the solubility of oxygen is lower in solutions with high ionic strength.

The scattered excitation light can be used as an indicator. If any gas is not dissolved in the electrolyte, bubbles occur in the cuvette and increase the intensity of scattered light. For reproducibility, the LED was always driven with a constant current of 500 mA.

This experimental setup was tested by anodic oxygen evolution at a platinum electrode. The fluorescence intensity of the dye is inversely proportional to the consumed charge for oxygen evolution on platinum, which can be easily measured and be used for calibration plots to quantify the amount of oxygen evolution in other electrochemical systems.

Results

Ta wires show the typical plateau current in cyclovoltammograms up to some 10 V. The statistical spikes of dielectric break-down and re-passivation are observed. The cyclovoltammograms of sintered Ta anodes (Fig. 5) are very similar up to 8 V, but then the shape changes completely. Oscillations of the current between zero and some milliampere per square centimeter were observed, accompanied by an alternating strong gas evolution (Fig. 6).

The oscillation frequency is influenced by the sweep rate which will be discussed later. The mechanism is obvious: gas bubbles develop and block the inner surface of the sintered cube, the current goes down to almost zero, as the outer surface of the sintered body, which still has electrolyte contact, is much smaller (some square millimeter) compared to the complete surface (some 100 cm^2). Then the gas bubbles leave the sintered body or dissolve in the electrolyte. The potential increased during the blocking period without further oxide growth, which is now accelerated and forms the current peak. Gas is evolved in parallel and a new cycle starts.

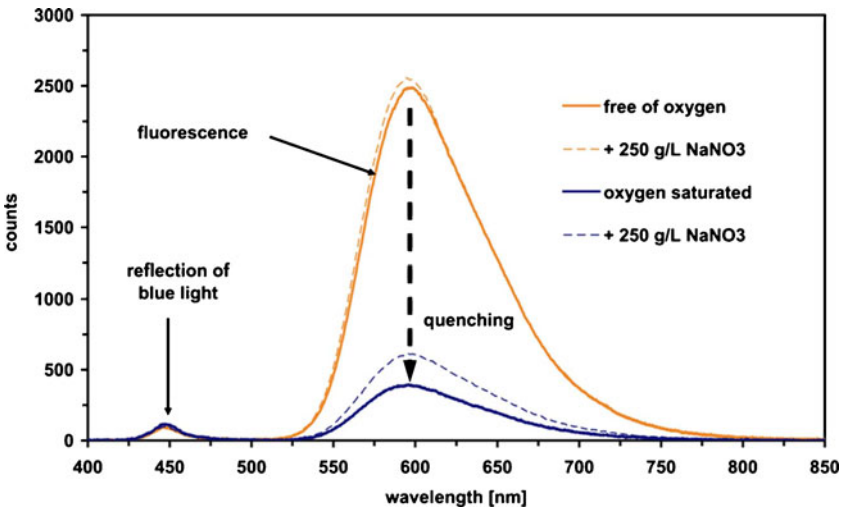

Fig. 4 Fluorescence quenching of 0.1 g L^{-1} dichlorotris(1, 10-phenanthroline)ruthenium(II) hydrate, (98%) by dissolved oxygen

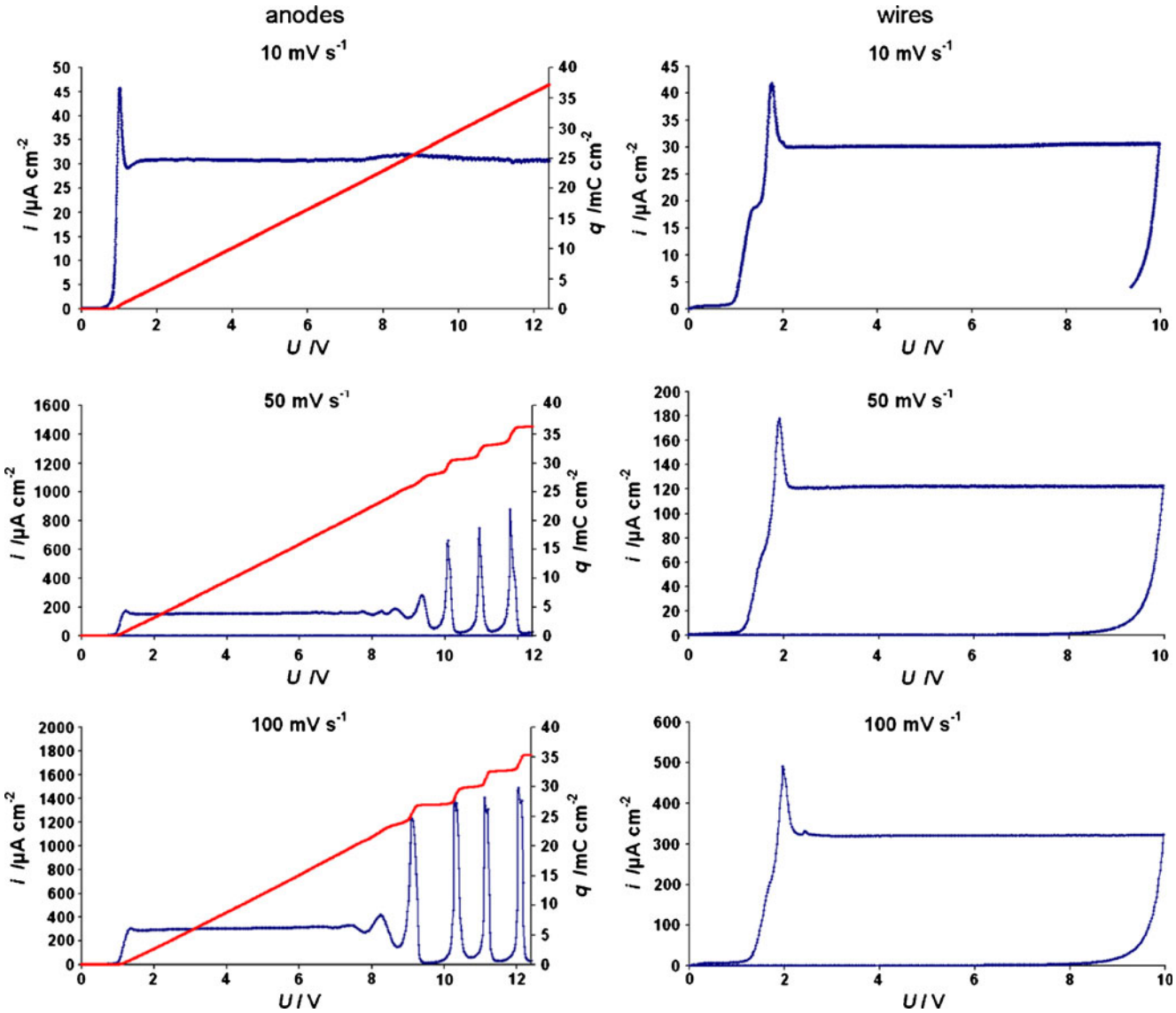

Fig. 5 Current density (*blue*) and corresponding charge (*red*) of sintered Ta anodes and cyclovoltammograms of wires with sweep rates of 10, 50, and 100 mVs^{-1}

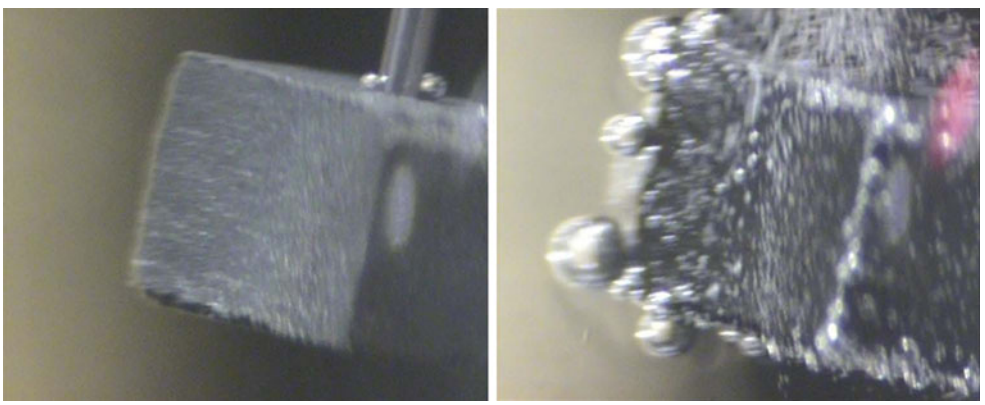

Fig. 6 Sintered Ta anode during cyclovoltammogram (sweep rate 100 mVs^{-1}) at potentials <9 V during blocking (*left*) and with gas evolution (*right*)

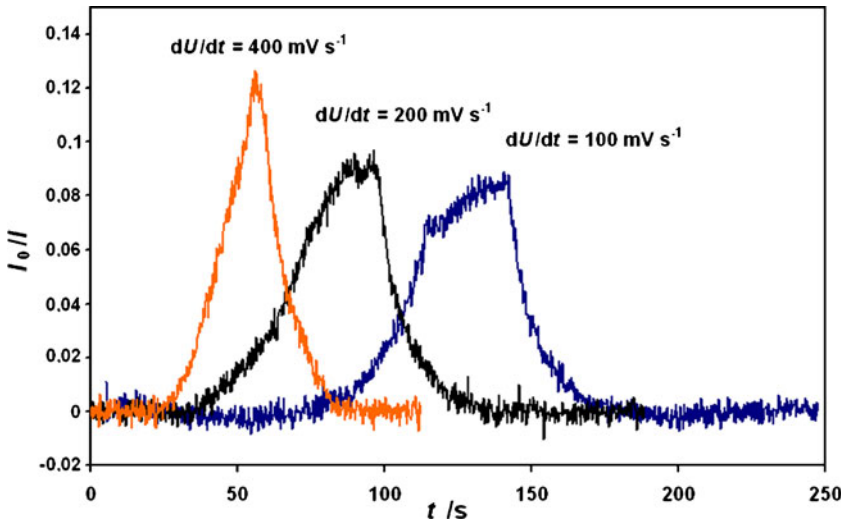

Fig. 7 Fluorescence quenching of dichlorotris(1,10-phenanthroline)ruthenium(II) hydrate during anodization with different sweep rates. Due to the very small amounts of gas, our detection by fluorescence quenching were limited to sweep rates >50 mVs^{-1}

The corresponding charge was calculated by numeric integration of the current. The mean slope does not change in the oscillation region, indicating that most of the charge is consumed for oxide formation. This fits to former results with current efficiencies close to 1. A first estimate of oxygen current density yielded some microampere per square centimeter. This is too small to be observed at wires, as the oxygen dissolves in the electrolyte and leaves the electrode by diffusion. Visible bubble formation requires current densities >1 $mAcm^{-2}$. The bubble formation at the sintered Ta anodes is an effect of the large inner surface and, thus, of super saturation of the gas.

Next step was an identification and quantification of the gas. Figure 7 and Table 1 show the results. Oxygen evolution requires an electronic conductivity of the oxide film (Eq. 3). If this conductivity is a common solid state property of the oxide, the oxygen amount should be proportional to the period of time within this potential limits and, therefore, increase with decreasing sweep rate, independently of the oxide formation current density. In fact, the oxygen amount is independent of the sweep rate. In the range from 100 to 400 mVs^{-1}, the amount does not decrease by a factor of 4 but remains almost constant.

Accordingly, cyclovoltammograms with 10 mVs^{-1} show no oscillations or bubble formation. The constant amount of gas is now distributed over a very long period of time and can be removed by diffusion without bubble formation.

Table 1 Charge of oxygen evolution and oxide formation

	100 mVs^{-1}	200 mVs^{-1}	400 mVs^{-1}
Q_{O2}/mC	208	192	142
Q_{total}/mC	4,718	5,021	3,734
Q_{O2}/Q_{total}	4.4%	3.8%	3.8%

Discussion

The oxygen amount is independent of the sweep rate, i.e., the oxygen amount is not dependent on the time in a specific voltage region and, therefore, the electronic conductivity is no intrinsic property of the oxide. The only parameter which is constant in that potential interval is the amount of oxide, as the formation factor k (Eq. 10) is only weakly dependent on the sweep rate. So we can assume that the amount of oxygen is coupled to the amount of oxide, which was formed at the same time, i.e.,

$$i_{O2} = f \cdot i_{Ox} \tag{13}$$

with a factor f which is around 0.04 (Table 1).

To explain this, we developed a model presented in Fig. 8. The oxide growth requires mobile ions, which produce transient states in the band gap (shaded area in

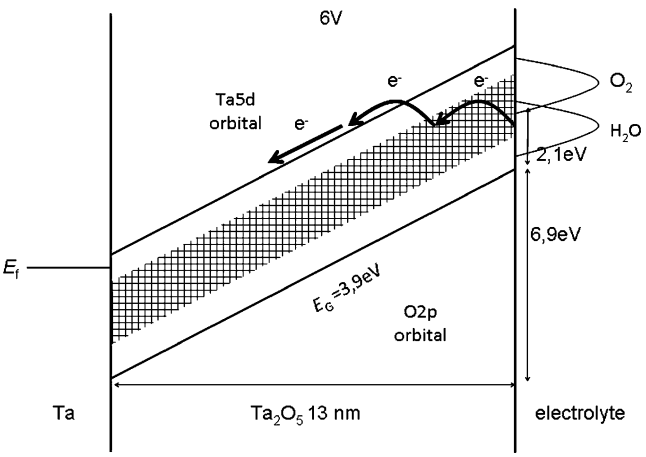

Fig. 8 Semi-quantitative band model of anodic Ta oxide. Mobile ions (oxygen?) form terms within the band gap of 3.9 eV during growth and enable electron tunneling [13]

Fig. 8). Electrons can cross the band gap by resonance tunneling, enter the conduction band, and move to the metal. The number of the interband states will increase with the growth rate and, thus, sweep rate, but the time within this oxygen region will decrease at the same time. These effects compensate each other and, as a result, the amount of oxygen remains constant.

From Fig. 8, one would conclude that this process should be possible at all potentials >3 V, but, in fact, bubbles are not formed at potentials <6 V. To explain this, we have to respect the porous structure of the anode. The mean pore diameter is around 100 nm. A formation of such tiny bubbles with a radius r depends on the surface tension of the electrolyte (σ=0.075 $\mathrm{N\,m^{-1}}$) and requires a large excess pressure Δp, which is given by the *Laplace* equation, ($\sigma = 0.075\ \mathrm{N\ m^{-1}}$), and requires a large excess pressure Δp, which is given by the *Laplace* equation:

$$\Delta p = \frac{2\sigma}{r} \approx 30\,\mathrm{bar} \tag{14}$$

The electrolyte volume in the anode is around $1.6 \cdot 10^{-9}$ $\mathrm{m^3}$. To build up such excess pressure, the concentration of supersaturated oxygen is calculated from *Henry's* law

$$c = \frac{p}{k} = \frac{30\ \mathrm{bar}}{770\ \mathrm{L\ bar\ mol^{-1}}} = 0.039\ \mathrm{mol\ L^{-1}} \tag{15}$$

and, inside the anode

$$39\ \mathrm{mol\ m^{-3}} \cdot 1.6 \cdot 10^{-9}\ \mathrm{m^3} = 6.2 \cdot 10^{-8}\ \mathrm{mol\ oxygen}$$

which corresponds to a charge of

$$Q_{\mathrm{supersat}} = 4 \cdot 96485\ \mathrm{C\ mol^{-1}} \cdot 6.2 \cdot 10^{-8}\ \mathrm{mol} = 24\ \mathrm{mC}$$

Bubble formation starts at sweep rates >20 $\mathrm{mV\,s^{-1}}$, this corresponds to currents of 14 mA. Assuming that 4% of the total current form oxygen, we get an equivalent of >560 $\mu\mathrm{C\ s^{-1}}$, which is dissolved and removed by diffusion. At 50 $\mathrm{mV\,s^{-1}}$ a total oxygen charge of

$$Q_{\mathrm{oxygen}} = 1.4\ \mathrm{mA} \cdot 60\ \mathrm{s} = 84\ \mathrm{mC}$$

is consumed between 3 and 6 V. Meanwhile, a charge

$$Q_{\mathrm{diffusion}} = 0.56\ \mathrm{mA} \cdot 60\ \mathrm{s} = 34\ \mathrm{mC}$$

is lost by diffusion. The remaining charge

$$Q_{\mathrm{oxygen}} - Q_{\mathrm{diffusion}} = 50\ \mathrm{mC}$$

is in the same order of magnitude as Q_{supersat}. This fits well, if we respect the uncertainties, especially the distribution of pore size.

Summary

Valve metals such as Al, Ta, or Nb cover with oxide films in a humid environment, which are similar to ceramics due to their large band gap. They should be perfect insulators for electron transport and, therefore inhibit oxygen evolution.

In industry, however, large amounts of gas are evolved during the anodization of tantalum anodes for electrolytic capacitor fabrication.

We detected the oxygen evolution at Ta anodes quantitatively by fluorescence quenching in a flow-through cuvette. The current efficiency of the oxide formation is about 96%, i.e., around 4% of the anodic charge is consumed for oxygen evolution. At common electrodes such as wires or sheets, this oxygen is removed by diffusion without bubble formation and, thus, not recognized. Due to the large inner area of the anodes, the oxygen evolution causes strong oscillations of the current density and bubble formation. This process is a cyclic formation of gas bubbles, blockage of the inner surface, removal of gas, further oxide growth, and back again.

The amount of oxygen is proportional to the oxide amount formed in parallel. Therefore, we assumed that mobile ions necessary for growth form interband states which allow electron tunneling through the oxide film. Accordingly, stationary no oxygen evolution is observed. The formation of gas bubbles within the tiny pores requires a significant super saturation and excess pressure which causes a delay of the oscillations in cyclovoltammograms by some Volts.

References

1. Kerrec O, Devillier D, Groult H, Chemla M (1995) Electrochim Acta 40:719
2. Young L (1954) Trans Faraday Soc 50:153
3. Lohrengel MM (2004) Untersuchungen der elektrochemischen Deckschichtkinetik mit Transientenmethoden. Shaker, Aachen
4. Vetter KJ (1967) Electrochem Kinet. Academic, New York, p 753
5. Macagno V, Schultze JW (1984) J Electroanal Chem 180:157
6. Van Rysselberghe P, Johansen HA (1959) J Electrochem Soc 106:355
7. Kumagai S, Young L (1964) J Electrochem Soc 111:1411
8. Klerer J (1965) J Electrochem Soc 112:896
9. Young L (1958) Proc Roy Soc 244:41
10. Mead CA (1972) In: Diggle JW (ed) The anodic behavior of metals and semiconductors. Dekker, New York, pp 287–318
11. Smith DJ, Young L (1983) Thin Solid Films 101:11
12. Walther B, Schneider M, Michaelis A, Lohrengel MM (2007) Electrochemical machining of Ti-based hard metal alloys. Conference transcript International Symposium on Electro Chemical Machining Technology INSECT 2007, Chemnitz, pp 35–40
13. Chun WJ, Ishikawa A, Fujisawa H, Takata T, Kondo JN, Hara M, Kawai M, Matsumoto Y, Domen K (2003) J Phys Chem 107:1798–1803